

1 **Antifungal activity of silver nanoparticles during *in-vitro* culture of *Stevia rebaudiana* Bertoni**

2 Marco A. Ramírez-Mosqueda¹ · Lino Sánchez-Segura² · Sandra L. Hernández-Valladolid³ · Elohim Bello-Bello⁴ ·

3 Jericó J. Bello-Bello^{5*}

4

5 ¹ Colegio de Postgraduados Campus Córdoba, Km. 348 de la Carretera Federal Córdoba-Veracruz, Congregación

6 Manuel León, Amatlán de los Reyes, Veracruz, Mexico

7 ² Departamento de Ingeniería Genética, Unidad Irapuato, CINVESTAV-Irapuato. Libramiento Norte

8 Carr. Irapuato-León Km 9.6. Irapuato, Guanajuato, México.

9 ³ Agricultura Sustentable y Protegida, Universidad Tecnológica del Centro de Veracruz, Av. Universidad 350, Dos

10 caminos, 94910 Cuitláhuac, Veracruz, Mexico

11 ⁴ Laboratorio Nacional de Genómica para la Biodiversidad/Unidad de Genómica Avanzada, Centro de Investigación

12 y Estudios Avanzados, Instituto Politécnico Nacional, 36821. Irapuato, Guanajuato, México.

13 ⁵ CONACYT-Colegio de Postgraduados Campus Córdoba, Km. 348 de la Carretera Federal Córdoba-Veracruz,

14 Congregación Manuel León, Amatlán de los Reyes, Veracruz, Mexico

15

16 * Authors for correspondence JJBB (jericobello@gmail.com)

17

18 Tel.: + 52 (271) 71 6 60 00

19

20

21

22

23

24

25

26

27

28

29 **Abstract**

30 Contamination by fungi and bacteria during the *in-vitro* propagation of plants leads to considerable losses of biological
31 material and precludes phytosanitary certification. The anti-microbial effect of silver nanoparticles (AgNPs) may be
32 an alternative for the eradication of *in-vitro* contaminants. This study evaluated the microbicidal activity of AgNPs on
33 a recurrent fungus during the micropropagation of stevia (*Stevia rebaudiana* Bertoni). First, the fungus was isolated
34 and identified at a molecular level by the sequencing and analysis of the ITS4/ITS5 rDNA region. The results of the
35 phylogenetic analysis of various fungi species showed that the strain under study (16-166-H) belongs to the genus
36 *Sordaria* and is 86.74% similar to *S. tomento-alba* (strain CBS 260.78). Subsequently, the inhibition of the growth of
37 *S. tomento-alba* was tested under different concentrations of AgNPs (0, 25, 50, 100, and 200 mg L⁻¹), observing that
38 50 and 100 mg L⁻¹ achieve ca. 50% growth inhibition (IC₅₀), while 200 mg L⁻¹ produces a drastic inhibition. On the
39 other hand, the shape and size of AgNPs was examined using transmission electron microscopy (TEM), and the
40 transport and accumulation of AgNPs in *S. tomento-alba* cells were monitored through multiphoton microscopy. The
41 morphological and fluorescence analyses showed that AgNPs display different sizes, with larger nanoparticles retained
42 in fungal cell walls while smaller AgNPs penetrate into fungal cells. Probably, apoplastic and symplastic mechanisms
43 involved in the accumulation and transport of AgNPs affect the metabolic processes of the fungus, thus inhibiting its
44 growth. These results suggest that AgNPs possess antifungal activity and can be used in the eradication of contaminants
45 during the *in-vitro* culture of plant species.

46

47 **Key words:** nanobiotechnology, silver nanoparticles, transmission electron microscopy, antifungal activity.

48

49

50

51

52

53

54

55

56

57

58

59

60

61 **Introduction**

62 Plant tissue culture (PTC) is a biotechnological technique used for the *in-vitro* conservation, handling, sanitation, and
63 propagation of edible, medicinal, and ornamental plants. *In-vitro* propagation, or micropropagation, represents a
64 commercial alternative to produce pathogen-free plants (Efferth 2019). The success of micropropagation depends on
65 ensuring strict asepsis. However, microbial contamination may occur during the micropropagation of plants, leading
66 to important losses of plant material *in vitro* (Medjemem et al. 2016).

67
68 PTC contamination may be due to endophyte microorganisms, anthropogenic factors, tolerance of microorganisms to
69 autoclaving, and resistance to antibiotics and fungicides (Thomas et al. 2017; Chechi et al. 2019; Marjon et al. 2019).
70 *In-vitro* contaminants can affect the growth of explants by competing for water, light, space, and essential nutrients
71 (Javed et al. 2017; Khan et al. 2018). In addition, the presence of contaminants limits the phytosanitary certification
72 of PTC plant material (Sastry et al. 2014; Whattam et al. 2014). Phytosanitary certification is a priority issue in
73 government policies in relation to economic income from the exportation and importation of *in vitro* plants of
74 commercial interest (Whattam et al. 2014; Eschen et al. 2015).

75
76 There are several techniques for contamination control in micropropagated plants. One of them involves the
77 treatment of parent plants and explants by adding fungicides and antibiotics to the culture medium (Cassells 2012).
78 Nonetheless, the addition of antibiotics or fungicides to the culture medium for controlling bacterial contamination is
79 not recommended due to the resistance of some strains (Caniça et al. 2019; Chechi et al. 2019). Biofilms with
80 microbicidal effect are also available and can be used to prevent contamination, such as Plant Preservative Mixture®
81 (PPM) and Vitrofur® (G1); however, their limited availability restrain their commercial application. An alternative
82 for the eradication of *in-vitro* contaminants is the use of silver nanoparticles (AgNPs). These have been used as
83 antimicrobial agents for the *in-vitro* culture of various plant species (Spinoso-Castillo et al. 2017; Tung et al. 2018).
84 The mechanisms of action of AgNPs as antifungal agent have not been fully elucidated because most studies have
85 addressed antiviral and antibacterial properties (Pařil et al. 2017; Khezerlou et al. 2018).

86
87 The culture of Stevia (*Stevia rebaudiana* Bertoni) is of high commercial value because of the non-caloric steviosides
88 and rebaudiosides contained in its leaves (Debnath et al. 2019; Rouhani et al. 2019). The commercial propagules
89 currently produced are insufficient given the low percentage of seed germination and the reduced number of cuttings

90 that adapt to soil (Angelini et al. 2018). The *in-vitro* propagation of this species is affected by spontaneous
91 contamination after its establishment and during subculture. For this reason, it is necessary to develop
92 micropropagation systems for this species to ensure the production of plants that are free of diseases and pathogens.
93 The objective of this study was the identification and control of contamination during the *in-vitro* establishment of *S.*
94 *rebaudiana* using silver nanoparticles.

95

96 **Materials and Methods**

97 *Physicochemical characterization of silver nanoparticles by transmission electron microscopy*

98 The AgNPs used in this study, formulated as Argovit[®], were provided by the Production Centre Vector-Vita Ltd,
99 located in Novosibirsk, Russia. Argovit[®] is made up of 12 mg mL⁻¹ of metallic silver and 188 mg mL⁻¹ of
100 polyvinylpyrrolidone (PVP, 15-30 kD). The morphology of nanoparticles was examined under a Philips/FEI
101 Morgagni M-268 transmission electron microscope (Brno, Czech Republic). For the morphological analysis, 5 µL of
102 particles in suspension were mounted on a copper grid of Formvar 300 mesh/carbon (Electron Microscopy Science,
103 PA). Samples were dried at room temperature for 5 min. The operating conditions in all experiments were: high
104 voltage (EHT) of 80 kV, high magnification of 1000-140000X, and working pressure of 5 x 10⁻³ Pa (5 x 10⁻⁵ Torr).
105 Micrographs were captured in tagged image file (.tif) format with a resolution of 1376 x 1032 pixels and a grey
106 scale. In this format, 0 was assigned to black and 255 to white in the grey scale.

107

108 *Plant Material*

109 The explants used were nodal segments of stevia (*Stevia rebaudiana* Bertoni cv. Morita II) measuring 2 cm in length
110 that contained one axillary bud. The explants were disinfected with a surfactant solution (Tween-20/distilled water)
111 and washed with a slow flow of running water for 30 minutes. Subsequently, in a laminar flow hood, explants were
112 immersed in 70% (v/v) ethanol for 30 s and in 0.6% and 0.3% (v/v) sodium hypochlorite for 10 and 5 min,
113 respectively. Three rinses with sterile water were performed. Finally, the explants were transferred to test tubes
114 containing MS medium (Murashige and Skoog 1962), supplemented with 1 mg L⁻¹ BA (Bencilademina, Sigma-
115 Aldrich, St. Louis, MO), 30 g L⁻¹ sucrose, and 2.5 g L⁻¹ Phytigel[™] (Sigma-Aldrich, St. Louis, MO). The pH of the
116 media was adjusted to 5.8 ± 0.2. The tubes with culture medium were autoclaved at 124 KPa for 15 min. Cultures
117 were incubated at 25 ± 2 °C with a 16/8 h photoperiod (light/dark), under an irradiation of 40-50 µmol m⁻² s⁻¹
118 provided by fluorescent lamps. Subsequently, the explants showing evidence of contamination were isolated.

119 *Isolation and culture of the fungus Sordaria tomento-alba*

120 Discs with mycelia from contaminated explants were transferred with a scalpel to Petri dishes containing potato
121 dextrose agar medium (PDA) (Sigma-Aldrich, St. Louis, MO). Subsequently, these discs were incubated at 27 °C for
122 72 hours.

123

124 *Molecular identification of contaminating microorganisms*

125 *DNA extraction, PCR amplification, and ITS sequencing*

126 Genomic DNA was extracted from fungal mycelium using an alkaline lysis method (Doyle and Doyle 1987). DNA
127 quality was measured using a Nanodrop® ND-1000 spectrophotometer (Thermo Scientific, Wilmington, USA).

128 Polymerase chain reaction (PCR) was performed using universal internal transcribed spacers (ITSs): ITS4 (5'-
129 TCCTCCGCTTATTGATATGC-3') and ITS5 (5'-GGAAGTAAAAGTCGTAACAAGG-3') primers (White *et al.*

130 1990). The PCR final volume of the reactions was 20 µl, containing 50 ng of genomic DNA, 1X of PCR buffer

131 (Invitrogen, EU), 0.8 mM of dNTPs (Invitrogen, EU), 3 mM MgCl₂, 0.5 µM of each primer and 1 U of *Taq* DNA

132 Polymerase (Invitrogen, EU). DNA amplification was performed in a GeneAmp® PCR System 9700 thermal cycler

133 (Perkin-Elmer). PCR parameters consisted of one cycle of initial denaturation at 90 °C for 30 s, followed by 35

134 cycles of denaturation at 90 °C for 15 s, primer annealing at 56 °C for 30 s, elongation at 72 °C for 1 min, and a final

135 elongation at 72 °C for 7 min. The amplification products were separated by electrophoresis in 1.2% (w/v) agarose

136 gel previously stained with ethidium bromide. The run was performed in TAE 1X buffer (Tris-Acetic acid-EDTA) at

137 100 V for 45 min. PCR products were sequenced at the Colegio de Postgraduados (Campus Montecillo) using the

138 HiSeq 2500® Sequencing System – Illumina (Sanger method). PCR products were sequenced at the Colegio de

139 Postgraduados (Campus Montecillo) using the HiSeq 2500® Sequencing System – Illumina (Sanger method).

140 *Multiple sequence alignment and phylogenetic tree construction*

141 ITS4/ITS5 rDNA from the 16-166-H strain was used as query sequence and compared against the NCBI database

142 using the BLAST nucleotide search tool (<https://blast.ncbi.nlm.nih.gov/Blast.cgi>) (Altschul *et al.*, 1997). An *in-silico*

143 analysis was developed with 15 target sequences producing significant alignments, using the *Colletotrichum*

144 *acutatum* (MH865675) sequence as outgroup control. The multiple sequence alignment was performed using the

145 ClustalW algorithm in the msa package (version 1.16.0) from the R program (Bodenhofer *et al.* 2015). For the

146 phylogenetic analysis, the ape package (version 5.3) was employed (Paradis and Schliep 2019). The phylogenetic

147 relations of samples were constructed using the Neighbor-Joining method, and the genetic distances were computed
148 using the Jukes-Cantor method (Jukes and Cantor 1969; Saitou and Nei 1987). The optimal tree was generated with
149 1000 bootstrap replicates. Bootstrap support threshold equal or greater than 50% was considered significant.
150 Graphical tree representation was plotted with the ggtree package (Yu et al 2017).

151

152 *Inhibition of fungal growth*

153 The antimicrobial activity of AgNPs on the growth of *S. tomento-alba* was explored using mycelia seeded in plates
154 with PDA and evaluating different concentrations of AgNPs (0, 25, 50, 100, and 200 mg L⁻¹). First, the culture
155 medium was adjusted to a pH of 6.5 and was sterilized at 124 KPa por 15 min. Then, all treatments were inoculated
156 with 1 cm² of fresh mycelium of *S. tomento-alba* and incubated under a photoperiod of 18/6 hours of light/darkness,
157 at 23-25 °C. After 5 days of incubation, the variable to measure was fungus growth in diameter (known as GD), with
158 the average of three measurements (in cm) considered as GD. The growth of *S. tomento-alba* was evaluated after 21
159 days of incubation.

160

161 For the fungus growth in diameter (cm), a completely randomized design was used, as described below:

162

$$163 \quad y_{ij} = \mu + conc_i + rep(conc)_{j(i)} + \varepsilon_{ij}$$

164

165 Where y_{ij} is fungus diameter observed at concentration i of AgNPs in replicate j ; μ is the overall mean; $conc_i$ is the
166 fixed effect of concentration i of AgNPs; $rep(conc)_{j(i)}$ is the random effect of replicate j nested on concentration i
167 of AgNPs assuming $rep(conc)_{j(i)} \sim N(0, \sigma_{rep(conc)}^2)$; and ε_{ij} is the experimental error with $\varepsilon_{ij} \sim N(0, \sigma^2)$. Fungus
168 growth was analyzed with the procedure PROC GLIMMIX of SAS (version 9.4) under a Generalized Linear Mixed
169 Model with Poisson distribution, and for fungus growth, Linear Mixed model was used.

170

171 *Detection and action of AgNPs in fungal inhibition by fluorescence microscopy*

172 AgNPs were detected using modifications of the "Lambda" method for determining the native spectral emission of
173 AgNPs (Castro-González et al. 2019). The nanoparticles accumulated in hyphae were visualized with a multiphoton
174 microscopy system (Axio Imager Z2, LSM 880-NLO, Zeiss, Oberkochen, Germany) coupled to a Ti: Sapphire

175 infrared laser (Chameleon Vision II, COHERENT, Santa Clara, CA, USA) with a tuning capability in the range of
176 690 to 1060 nm. In all experiments, the operating conditions involved the use of a Chameleon laser set at 850 nm
177 with 1.5% power, pinole at 600.1, and similar photodetector voltage ranges. Emissions from AgNPs were recovered
178 at 596–637 nm. Images of hyphae were captured with a 63X/1.40 immersion objective, and NA ∞-0.17, using a
179 Zeiss Plan NEOFLUAR with a 5 nm spectral sensitivity. All micrographs were captured in CZI format in a size of
180 1131x1131 pixels composed of three color channels (RGB).

181

182 **Results**

183 *Physicochemical characteristics of Argovit®*

184 The physicochemical characteristics of AgNPs are shown in Table 1. The AgNPs characterized by TEM are
185 spherical with a form factor of (0.82) and roundness of 0.88. The analysis of AgNP dimensions showed average
186 diameters of 35 ±15 nm, which consists of clustered silver (12 mg/mL metallic silver) functionalized with 188
187 mg/mL of polyvinylpyrrolidone (PVP, 10-30 kD). The results obtained evidence the structural dimensions of AgNPs
188 (Argovit®-CP) in terms of shape and size. The size of AgNPs was verified by TEM, showing macroscopic aggregates
189 composed of silver nanoparticles. The TEM micrograph (Figure 1) corroborates the tendency to aggregate; NPs of
190 different sizes were observed, showing spheroidal nanoparticles ranging from 13 nm to 80 nm.

191

192 *Molecular identification of the 16-166-H fungal strain*

193 The BLAST algorithm-based analysis of the 560-bp ITS sequence showed that this fungal strain had a high percent
194 identity value (96.64%) to *Sordaria* strains JN207345, JN207271, and JN207268, which are associated to *Sordaria*
195 *tomento-alba* as reported by Loro et al. 2012. Moreover, these results were confirmed by the phylogenetic tree
196 analysis. The topology of the phylogenetic tree showed the formation of 5 clades. Among these clades, *Sordaria* and
197 *Asordaria* species were grouped in three internal clades (Fig. 2). Clade I comprises *Sordariomycetes* sp., *Sordaria*
198 *fimicola*, and *Sordaria fimicola*; Clade II comprises *Sordaria tomento-alba* and related *Sordaria* strains (including
199 16-166-H); finally, Clade III comprises *Sordaria* sp., *Asordaria prolifica*, and *Asordaria conoidea*. Both results
200 reveal insights into the molecular identification of the fungal isolate. For this analysis, a reference strain was
201 deposited in Genbank (<https://www.ncbi.nlm.nih.gov/genbank/>).

202

203 *Inhibition of fungal growth*

204 The results show the fungicidal effect of AgNPs on the growth of *S. tomento-alba* in solid culture medium. AgNP
205 concentrations of at least 50 mg L⁻¹ produced a significant inhibition on fungal growth (Fig. 3). The highest greatest
206 fungal GD was observed at 0 and 25 mg L⁻¹ NPsAg, with 7.00 ± 0.54 and 7.60 ± 0.34 cm in diameter, respectively,
207 whereas the lowest occurred at 200 mg L⁻¹, with 2.50 ± 0.05 cm (Fig. 4). For 50 and 100 mg L⁻¹, no significant
208 differences were observed in the development of the fungus, recording an average diameter of 4.30 ± 0.60 and $4.13 \pm$
209 0.41 cm, respectively. (Fig. 3).

210

211 *Detection and effect of AgNPs on fungal growth inhibition by fluorescence microscopy*

212 Multiphoton microscopy allowed observing the presence of AgNPs in fungus cells. It evidenced the presence of
213 AgNPs in the cell wall of hyphae (cross-section) subjected to the different treatments with NPs. However, as AgNP
214 concentration increased, nanoparticles showed a trend to accumulate in the space between the cell wall and the cell
215 membrane. The sequence of images in Fig. 5 shows the clear field and fluorescence of AgNPs and the progression of
216 fluorescence in stem cross-sections under different treatments with AgNPs.

217

218 **Discussion**

219 This study evidenced the antifungal effect of AgNPs on the fungus *S. tomento-alba* during the *in-vitro* establishment
220 of *S. rebaudiana*. *S. tomento-alba* has been reported as an endophyte in various plant species, including
221 *Stryphnodendron adstringens* (Carvalho et al. 2012), *Cenchrus ciliaris*, and *Cenchrus cf. spinifex* Cav. (Loro et al.
222 2012), and in different cultivars of *Solanum tuberosum* (Zimudzi et al. 2017). Although this fungus is not reported as
223 a phytopathogen, it causes contamination issues in *in-vitro* *Stevia* cultures. The effectiveness of AgNPs in the
224 elimination of microbial contaminants from *in-vitro* cultures depends on AgNP size, shape, and type of coating. With
225 regard to the characterization of Argovit[®], the TEM allowed us to observe particles of 40 ± 10 nm in size, with the
226 dominance of a spheroid form factor (0.80). The toxicity of AgNPs in biological systems has been reported to be
227 inversely proportional to particle size (i.e., smaller particles are more toxic) (Panzarini et al. 2018).

228 The analysis of the ITS sequence of the fungal strain 16-166-H supported its identification as belonging to the genus
229 *Sordaria*, genetically related to the species *S. tomento-alba*. The molecular identification of contaminants is relevant
230 because it allows knowing its origin and deriving an appropriate treatment for the disinfection of explants (Tomasi et

231 al. 2017). In this study, it was found that *S. tomento-alba* is a non-phytopathogenic endophyte. However, it can
232 lead to contamination in the *in-vitro* establishment of *S. rebaudiana* and, if uncontrolled, may spread across the
233 laboratory and affect other species cultured *in vitro*. The AgNPs used in this study probably affect the growth of
234 species of the genus *Sordaria* (*Sordaria* spp.). In general, *in-vitro* contaminants first use the carbon available
235 within the plant to survive; subsequently, they migrate to the culture medium that is rich in nutrients and
236 contains sucrose as carbon source. The fungi in the culture medium compete with explants for space, water,
237 light, and nutrients, causing the death of explants (Cassells 2012; Tomasi et al. 2017). One option to eradicate
238 these microorganisms is through the culture of meristems, thermotherapy, and use of antifungal agents
239 (Cassells 2012; Smith 2013; Sasi and Bhat 2018). The culture of meristems has been used primarily to eradicate
240 viruses (Sasi and Bhat, 2018); for its part, thermotherapy occasionally damages the explants (Hu et al. 2019; Kaur et
241 al. 2019). As regards the use of antifungal agents, these can lead to the development of resistance in some fungal
242 strains (Caniça et al. 2019; Chechi et al. 2019). AgNPs do not exert selective pressure on microorganisms and,
243 therefore, do not lead to resistance (Lemire et al. 2013; Khezerlou et al. 2018); thus, these may be less toxic than
244 synthetic fungicides.

245
246 In our study, during the inhibition of the growth of *S. tomento-alba*, we noted that AgNP concentrations of 50 and
247 100 mg L⁻¹ correspond to the half maximal inhibitory concentration (IC₅₀). An antifungal effect of AgNPs has been
248 reported for different fungi strains. Jo et al. (2009) mention that AgNP concentrations from 200 mg L⁻¹ were needed
249 to control the development of spores of *Bipolaris sorokiniana* and *Magnaporthe grisea*. On the other hand, Pulit et
250 al. (2013) demonstrated the inhibition of the growth of *Cladosporium cladosporioides* and *Aspergillus niger* strains
251 at 50 mg L⁻¹ AgNPs. Kim et al. (2009) observed that 25 mg L⁻¹ of AgNPs affect the integrity of the structure of
252 hyphae of *Raffaelea* spp., while Kasproicz et al., (2010) noted that 10 mg L⁻¹ of AgNPs reduce the radial growth of
253 *Fusarium culmorum*. Moreover, AgNP concentrations from 2.5 mg L⁻¹ drastically reduce the germination of spores.
254 Recently, Ruiz-Romero et al. (2018) used AgNPs to inhibit the radial growth of two phytopathogenic fungi
255 (*Fusarium solani* and *Macrophomina phaseolina*). However, this work only mentions that the AgNPs supplemented
256 were obtained as an extract from *Yucca* (*Yucca shilerifera*), without reporting the AgNP concentration. Also, the
257 physicochemical characteristics of AgNPs are not reported in the studies mentioned above. It is our opinion that
258 AgNPs should be characterized before conducting a research study.

259 The microbicidal effect of AgNPs derives from the interaction of silver ions with a broad range of molecular and
260 metabolic processes within organisms, including growth inhibition, cell death, and inhibition of DNA replication
261 (Abdi et al. 2008; Yun'an Qing et al. 2018). In fungi, AgNPs break the cell membrane of hyphae, thus impairing
262 infection mechanisms (Kim et al. 2008; Bocate et al. 2019) and inhibiting the germination of conidia (Kim et al.
263 2009). In our study, we observed the accumulation of AgNPs in the cell wall and cytoplasm of hyphae of *S. tomento-*
264 *alba*. The exact mechanism of transport and accumulation of AgNPs in fungi is currently unknown. However, the
265 results of the characterization of AgNPs suggest that due to diversity of sizes (2-85 nm), larger nanoparticles
266 accumulate in the cell wall and cell membrane, affecting the integrity of these organelles; for their part, smaller
267 nanoparticles penetrate through pores in the cell wall and the cell membrane via transport by plasmodesmata.
268 According to Money (1990), cell membrane pore size in hyphae of some fungi ranges from 2.3-3.3 nm, which could
269 explain the penetration of small nanoparticles. AgNPs that manage to penetrate inside the cell cause an increase of
270 Ag⁺ cations, which could affect the electrical potential of the membrane. According to Srikar et al. (2016) and
271 Khezerlou et al. (2018), these Ag⁺ ions denature proteins, deplete intracellular ATP, and form complexes with
272 DNA bases, so that the DNA loses its replication ability. On the other hand, the reaction of Ag⁺ with thiol,
273 carboxylate, phosphate, hydroxyl, amine, imidazole, and indole groups in enzymes may lead to their inactivation and
274 cell death (Lin et al. 1998; Ashraf et al. 2013). The Ag⁺ in nanoparticles probably exerts important effects on
275 biological systems. The use of AgNPs for disease control has the advantage of being non-toxic to humans and the
276 environment, unlike synthetic pesticides.

277
278 In conclusion, the AgNPs used in this study showed an antifungal effect in *S. tomento-alba*, a common contaminant
279 during the establishment of *S. rebaudiana*. AgNPs with similar physicochemical characteristics may be used to
280 control other fungal strains that contaminate *in-vitro* cultures. Therefore, further studies should be conducted on the
281 microbicidal potential of AgNPs in the micropropagation of different plant species, and the effects of AgNPs on
282 DNA damage and replication.

283

284 **Conflict of interest**

285 The authors declare that they have no conflicting interests.

286 **Author contribution statement**

287 SLH and JJBB devised and designed this research. SLH and LSS conducted the experiments. MARM and EBB
288 performed and reviewed the molecular and statistical analyses. MARM and JJBB drafted the manuscript. All authors
289 reviewed and approved the manuscript.

290

291 **References**

292 Abdi G, Salehi H, Khosh-Khui M (2008) Nano silver: a novel nanomaterial for removal of bacterial contaminants in
293 valerian (*Valeriana officinalis* L.) tissue culture. Acta Physiol Plant 30: 709-714.

294 <https://doi.org/10.1007/s11738-008-0169-z>

295 Altschul SF, Madden TL, Schaffer AA, Zhang J, Zhang Z, Miller W, Lipman DJ (1997) Gapped BLAST and PSI-
296 BLAST: a new generation of protein database search programs. Nucleic Acids Res 25:3389-3402.

297 <https://doi.org/10.1093/nar/25.17.3389>

298 Angelini LG, Martini A, Passera B, Tavarini S (2018) Cultivation of *Stevia rebaudiana* Bertoni and Associated
299 Challenges. In: Mérillon JM., Ramawat K. (eds) Sweeteners. Reference Series in Phytochemistry. Springer,
300 Cham. https://doi.org/10.1007/978-3-319-27027-2_8

301 Ashraf S, Abbasi AZ, Pfeiffer C, Hussain SZ, Khalid ZM, Gil PR, Parak WJ, Hussain I (2013) Protein-Mediated
302 Synthesis, pH-Induced Reversible Agglomeration, Toxicity and Cellular Interaction of Silver Nanoparticles.
303 Colloid Surf B-Biointerfaces 102 (2013) 511–51. <https://doi.org/10.1016/j.colsurfb.2012.09.032>

304 Bocatea KP, Reisa GF, de Souzaa PC, Oliveira Junior AG, Durán N, Nakazatoa G, Furlanetoa MC, de Almeida RC,
305 Panagio LA (2019) Antifungal activity of silver nanoparticles and simvastatin against toxigenic species of
306 *Aspergillus*. Int J Food Microbiol 291:79–86. <https://doi.org/10.1016/j.ijfoodmicro.2018.11.012>

307 Bodenhofer U, Bonatesta E, Horejš-Kainrath C, Hochreiter S (2015). msa: an R package for multiple sequence
308 alignment. Bioinformatics 31:3997-3999. <https://doi.org/10.1093/bioinformatics/btv494>

309 Caniça M, Manageiroa V, Abriouel H, Moran-Gilad J (2019) Antibiotic resistance in foodborne bacteria. Trends
310 Food Sci Technol. 84:41–44. <https://doi.org/10.1016/j.tifs.2018.08.001>

311 Carvalho CR, Gonçalves VN, Pereira CB, Johann S, Galliza IV, Alves TMA, Rabello A, Sobral MAG, Zani CL,
312 Rosa CA, Rosa LH (2012) The diversity, antimicrobial and anticancer activity of endophytic fungi
313 associated with the medicinal plant *Stryphnodendron adstringens* (Mart.) Coville (Fabaceae) from the
314 Brazilian savannah. Symbiosis 57:95–107. <https://doi.org/10.1007/s13199-012-0182-2>

- 315 Cassells A.C. (2012) Pathogen and Biological Contamination Management in Plant Tissue Culture: Phytopathogens,
316 Vitro Pathogens, and Vitro Pests. In: Loyola-Vargas V., Ochoa-Alejo N. (eds) Plant Cell Culture Protocols.
317 Methods in Molecular Biology (Methods and Protocols), vol 877. Humana Press, Totowa, NJ.
318 https://doi.org/10.1007/978-1-61779-818-4_6
- 319 Hu G, Dong Y, Zhang Z, Fan X, Ren F (2019) Elimination of apple necrosis mosaic virus from potted apple plants
320 by thermotherapy combined with shoot-tip grafting. *Sci Hortic* 252:310–315.
321 <https://doi.org/10.1016/j.scienta.2019.03.065>
- 322 Javed SB, Alatar AA, Basahi R, Anis M, Faisal M, Husain FM (2017) Copper induced suppression of systemic
323 microbial contamination in *Erythrina variegata* L. during *in vitro* culture. *Plant Cell Tissue Organ Cult*
324 128:249–258. <https://doi.org/10.1007/s11240-016-1104-4>
- 325 Jo YK, Kim BH, Jung G (2009) Antifungal Activity of Silver Ions and Nanoparticles on Phytopathogenic Fungi.
326 *Plant Dis* 93:1037-1043. <https://doi.org/10.1094/PDIS-93-10-1037>
- 327 Jukes TH and Cantor CR (1969). Evolution of protein molecules. In Munro HN, editor, *Mammalian Protein*
328 *Metabolism*, pp. 21-132, Academic Press, New York. <https://doi.org/10.1016/B978-1-4832-3211-9.50009-7>
- 329 Kasprovicz MJ, Koziol M, Gorczyca A (2010) The effect of silver nanoparticles on phytopathogenic spores of
330 *Fusarium culmorum*. *Can J Microbiol* 56:247–253. <https://doi.org/10.1139/W10-012>
- 331 Kaur C, Raj R, Kumar S, Purshottam DK, Agrawal L, Chauhan PS, Raj SK (2019) Elimination of Bean yellow
332 mosaic virus from infected cormels of three cultivars of gladiolus using thermo-, electro- and chemotherapy.
333 *3 Biotech* 9:154. <https://doi.org/10.1007/s13205-019-1684-x>
- 334 Khan T, Abbasi BH, Iqar I, Khan MA, Shinwari ZK (2018) Molecular identification and control of endophytic
335 contamination during *in vitro* plantlet development of *Fagonia indica*. *Acta Physiol Plant.* (2018) 40:150.
336 <https://doi.org/10.1007/s11738-018-2727-3>
- 337 Khezerlou A, Alizadeh-Sanib M, Azizi-Lalabadib M, Ehsanic A (2018) Nanoparticles and their antimicrobial
338 properties against pathogens including bacteria, fungi, parasites and viruses. *Microb Pathog* 123:505–526.
339 <https://doi.org/10.1016/j.micpath.2018.08.008>
- 340 Kim KJ, Sung WS, Moon SK, Choi JS, Kim JG, Lee DG (2008) Antifungal effect of silver nanoparticles on
341 dermatophytes. *J Microbiol Biotechnol* 18:1482-1484.

- 342 Kim SW, Kim KS, Lamsal K, Kim YJ, Kim SB, Jung M, Sim SJ, Kim HS, Chang SJ, Kim JK, Lee YS (2009) An In
343 Vitro Study of the Antifungal Effect of Silver Nanoparticles on Oak Wilt Pathogen *Raffaelea* sp. J
344 Microbiol Biotechnol 19:760–764. <https://doi.org/10.4014/jmb.0812.649>
- 345 Lemire JA, Harrison JJ, Turner RJ (2013) Antimicrobial activity of metals: mechanisms, molecular targets and
346 applications. Nat Rev Microbiol 11:371–384. <https://doi.org/10.1038/nrmicro3028>
- 347 Lin YE, Vidic RD, Stout JE, McCartney CA, Yu VL (1998) Inactivation of *Mycobacterium avium* by copper and
348 silver ions. Water Res 32:1997–2000. [https://doi.org/10.1016/S0043-1354\(97\)00460-0](https://doi.org/10.1016/S0043-1354(97)00460-0)
- 349 Loro M, Valero-Jimenez CA, Nozawa S, Marquez LM (2012) Diversity and composition of fungal endophytes in
350 semiarid Northwest Venezuela. J Arid Environ 85: 46-55. <https://doi.org/10.1016/j.jaridenv.2012.04.009>
- 351 Medjemem M, Harabi A, Bouzerara F, Foughali L, Boudaira B, Guechi A, Brihi N (2016) Elaboration and
352 characterization of low cost ceramics microfiltration membranes applied to the sterilization of plant tissue
353 culture media. J Taiwan Inst Chem Eng 59:79–85. <http://dx.doi.org/10.1016/j.jtice.2015.07.032>
- 354 Money NP (1990) Measurement of Pore Size in the Hyphal Cell Wall of *Achlya bisexualis*. Exp Mycol 14:234-242.
355 [https://doi.org/10.1016/0147-5975\(90\)90021-K](https://doi.org/10.1016/0147-5975(90)90021-K)
- 356 Murashige T, Skoog F (1962) A revised medium for rapid growth and bioassays with tobacco tissue cultures. Physiol
357 Plant 15:473–497. <https://doi.org/10.1111/j.1399-3054.1962.tb08052.x>
- 358 Panzarini E, Mariano E, Carata E, Mura F, Rossi M, Dini L (2019) Intracellular Transport of Silver and Gold
359 Nanoparticles and Biological Responses: An Update. Int J Mol Sci 19:305.
360 <https://doi.org/10.3390/ijms19051305>
- 361 Paradis E, Schliep K (2019). ape 5.0: an environment for modern phylogenetics and evolutionary analyses in R.
362 Bioinformatics 35:526-528. <https://doi.org/10.1093/bioinformatics/bty633>
- 363 Pařil P, Baar J, Āermá P, Rademacher P, Prucek R, Sivera M, PanáčĀ A (2017). Antifungal effects of copper and
364 silver nanoparticles against white and brown-rot fungi. J Mater Sci 52:2720–2729.
365 <https://doi.org/10.1007/S10853-016-0565-5>
- 366 Pulit J, Banach M, Szczygłowska R, Bryk M (2013) Nanosilver against fungi. Silver nano-particles as an effective
367 biocidal factor. Acta Biochim Pol 60:795–798. https://doi.org/10.18388/abp.2013_2060
- 368 Rouhani M (2019) Modeling and optimization of ultrasound-assisted green extraction and rapid HPTLC analysis of
369 stevioside from *Stevia Rebaudiana*. Ind Crop Prod 132:226–235.
370 <https://doi.org/10.1016/j.indcrop.2019.02.029>

- 371 Ruiz-Romero P, Valdez-Salas B, González-Mendoza D, Mendez-Trujillo V (2018). Antifungal Effects of Silver
372 Phytonanoparticles from *Yucca shilerifera* Against Strawberry Soil-Borne Pathogens: *Fusarium solani* and
373 *Macrophomina phaseolina*. *Mycobiology* 46:47-51. <https://doi.org/10.1080/12298093.2018.1454011>
- 374 Saitou N and Nei M (1987). The neighbor-joining method: A new method for reconstructing phylogenetic trees. *Mol*
375 *Biol Evol* 4:406-425. <https://doi.org/10.1093/oxfordjournals.molbev.a040454>
- 376 Sasi S, Bhat AI (2018) In vitro elimination of Piper yellow mottle virus from infected black pepper through somatic
377 embryogenesis and meristem-tip culture. *Crop Prot* 103:39-45.
378 <http://dx.doi.org/10.1016/j.cropro.2017.09.004>
- 379 Sastry KS, Zitter TA, Management of Virus and Viroid Diseases of Crops in the Tropics. In: Plant Virus and Viroid
380 Diseases in the Tropics. Springer, Dordrecht. https://doi.org/10.1007/978-94-007-7820-7_2
- 381 Smith RH (2013) Meristem Culture for Virus-Free Plants. In: Smith RH (ed) Plant Tissue Culture (Third Edition),
382 Academic Press, Pp. 119-126. <https://doi.org/10.1016/B978-0-12-415920-4.00011-6>.
- 383 Spinoso- Castillo JL, Chavez- Santoscoy RA, Bogdanchikova N, Perez- Sato JA, Morales- Ramos V, Bello- Bello JJ
384 (2017). Antimicrobial and hormetic effects of silver nanoparticles on in vitro regeneration of vanilla
385 (*Vanilla planifolia* Jacks. Ex Andrews) using a temporary immersion system. *Plant Cell Tissue Organ Cult*
386 129:195–207. <https://doi.org/10.1007/s11240-017-1169-8>
- 387 Srikar S, Giri D, Pal D, Mishra P, Upadhyay S (2016) Green Synthesis of Silver Nanoparticles: A Review. *Green*
388 *Sust Chem* 6:34-56. <http://dx.doi.org/10.4236/gsc.2016.61004>
- 389 Thomas P, Agrawal M, Bharathkumar CB (2017). Use of Plant Preservative Mixture™ for establishing *in vitro*
390 cultures from field plants: Experience with papaya reveals several PPMTM tolerant endophyticbacteria.
391 *Plant Cell Rep* 36:1717–1730. <https://doi.org/10.1007/s00299-017-2185-1>
- 392 Tung HT, Nam NB, Huy NP, Luan VQ, Hien VT, Phuong TTB, Le DT, Loc NH, Nhut DT (2018) A system for
393 large scale production of *chrysanthemum* using microponics with the supplement of silver nanoparticles
394 under light-emitting diodes. *Sci Hortic* 232:153–161. <https://doi.org/10.1016/j.scienta.2017.12.063>
- 395 Wells-Bennika MHJ, Janssen PWM, Klaus V, Yanga C, Zwietering MH, Den Bestenb HMW (2019) Heat
396 resistance of spores of 18 strains of *Geobacillus stearothermophilus* and impact of culturing. *Int J Food*
397 *Microbiol.* 291:161–172. <https://doi.org/10.1016/j.ijfoodmicro.2018.11.005>

398 Whattam M, Clover G, Firko M, Kalaris T (2014) The Biosecurity Continuum and Trade: Border Operations. In:
399 Gordh G., McKirdy S. (eds) The Handbook of Plant Biosecurity. Springer, Dordrecht.
400 https://doi.org/10.1007/978-94-007-7365-3_6
401 Yu G, Smith D, Zhu H, Guan Y, Lam TTY (2017). ggtree: an R package for visualization and annotation of
402 phylogenetic trees with their covariates and other associated data. *Methods Ecol Evol* 8:28-36.
403 <https://doi.org/10.1111/2041-210X.12628>
404 Zimudzi J, Coutinho TA, van der Waals JE (2017) Pathogenicity of Fungi Isolated from Atypical Skin Blemishes on
405 Potatoes in South Africa and Zimbabwe. *Potato Res* 60:119–144. [https://doi.org/10.1007/s11540-017-9345-](https://doi.org/10.1007/s11540-017-9345-0)
406 [0](https://doi.org/10.1007/s11540-017-9345-0)
407
408
409
410
411
412
413
414
415
416
417
418
419
420
421
422
423
424
425
426

427 **Tables**

Table 1. Physicochemical characteristics of Argovit®

Properties	Mean
Average diameter of metallic silver particles by TEM (nm)	40±10
Form Factor (Spheroid)	0.80
Metallic silver content (% wt.)	1.2
PVP Content (% wt.)	18.8
Roundness	0.80
Size interval of metallic silver particles by TEM (nm)	2 - 85
Zeta potential (mV)	-15

Abbreviations: Ag, silver; PVP, polyvinylpyrrolidone; TEM, transmission electron microscopy.

428
429
430
431
432
433
434
435
436
437
438
439
440
441
442
443
444
445

446 **Legends of figures**

447 **Fig. 1** Microphotographs of Argovit® AgNPs. a) Magnified TEM images of an AgNP aggregate of spherical shape
448 and several sizes in the range of 36.59-66.24 nm. Scale bar=100 nm. b) TEM micrograph of AgNP aggregates. Scale
449 bar = 500 nm.

450
451 **Fig. 2** Phylogenetic tree and multiple sequence alignment of 16-166-H strain based on ITS4/ITS5 rDNA and NCBI
452 BLAST sequences. A) The phylogenetic tree was inferred from a distance analysis with the Neighbor-Joining method.
453 *Colletotrichum acutatum* (MH865675) was used as outgroup. B) An abstract multiple sequence alignment of 16 NCBI
454 BLAST sequences was performed with the ClustalW algorithm. Numbers at the top of the graph correspond to columns
455 in the alignment (bp). Nucleotide legends are shown at the bottom.

456
457 **Fig. 3** Effect of different AgNP concentrations on growth of *Sordaria tomento-alba* in PDA medium after 21 days.
458 Bars represent the mean \pm standard error. Bars followed by different letters denote significant statistical differences
459 (Tukey, $p \leq 0.05$).

460
461 **Fig. 4** Growth of *S. tomento-alba* in PDA supplemented with different concentrations of AgNPs after 21 days of
462 incubation: a) 0 mg L⁻¹, b) 25 mg L⁻¹, c) 50 mg L⁻¹, d) 100 mg L⁻¹, and e) 200 mg L⁻¹.

463
464 **Fig. 5** Location of AgNPs in *S. tomento-alba* cultured in PDA media. a-b) 0 mg L⁻¹ AgNPs, merging and fluorescence,
465 respectively, c-b) 200 mg L⁻¹ AgNPs, merging and fluorescence, respectively. Bar = 10 μ m.

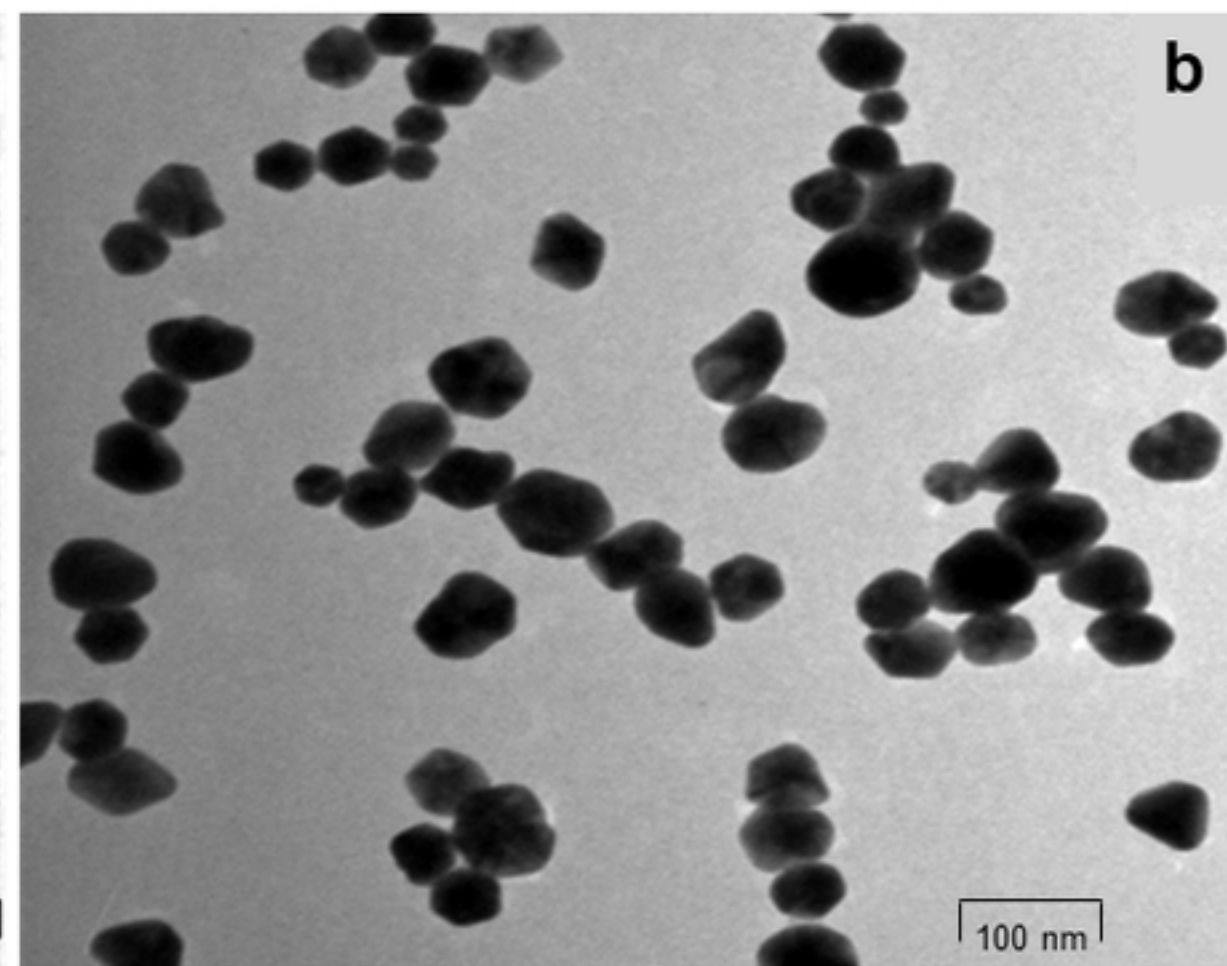
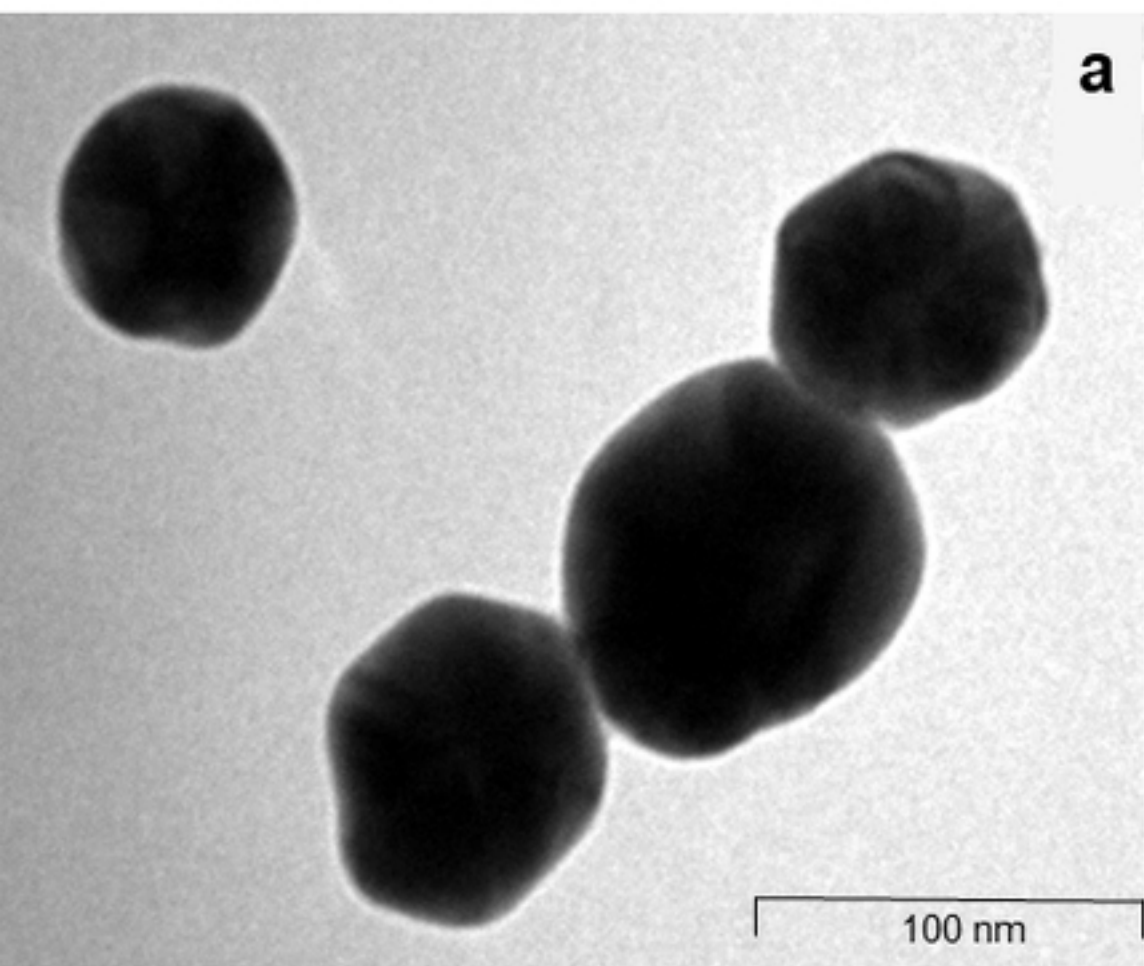


Figure 1

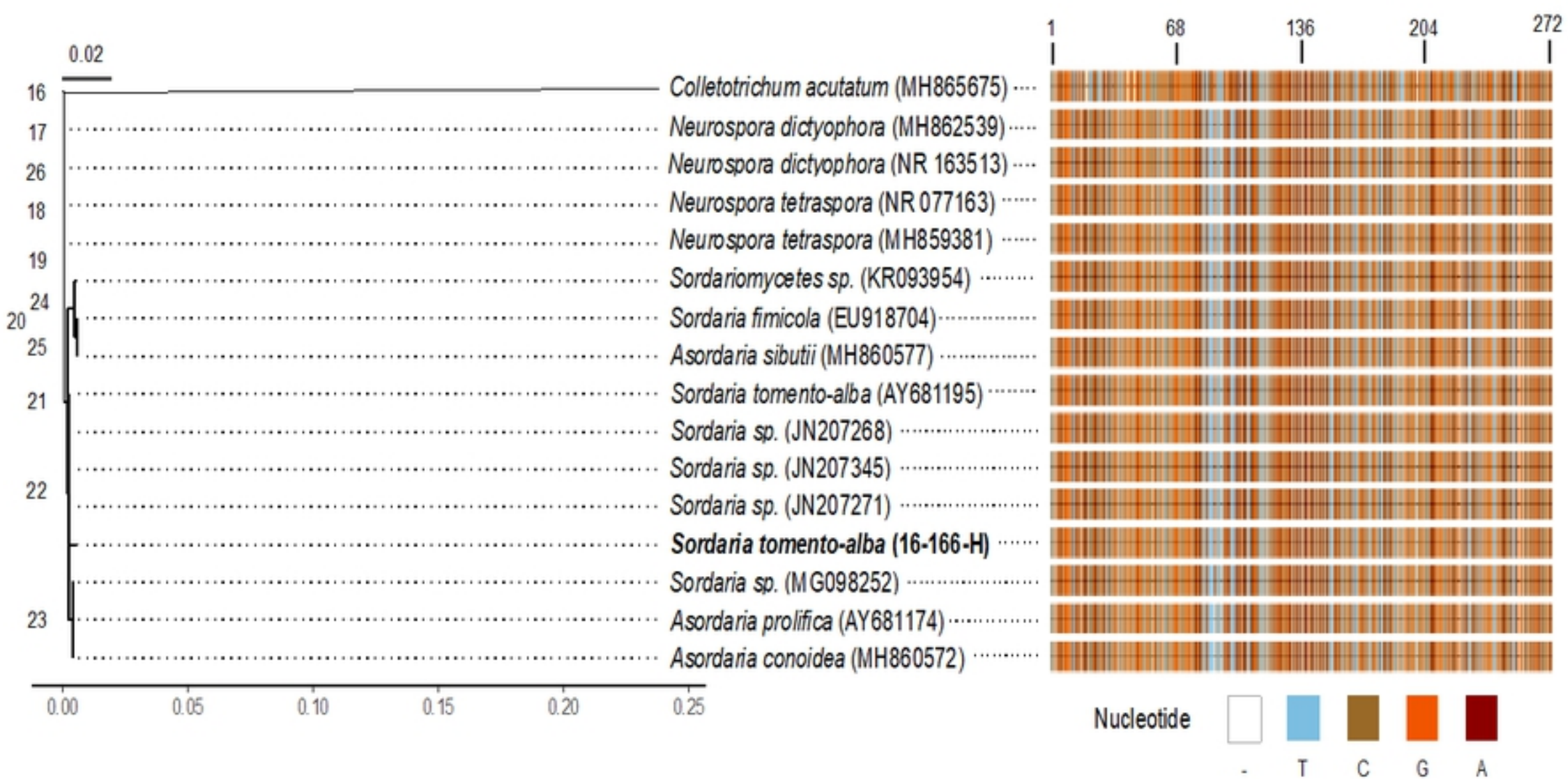


Figure 2

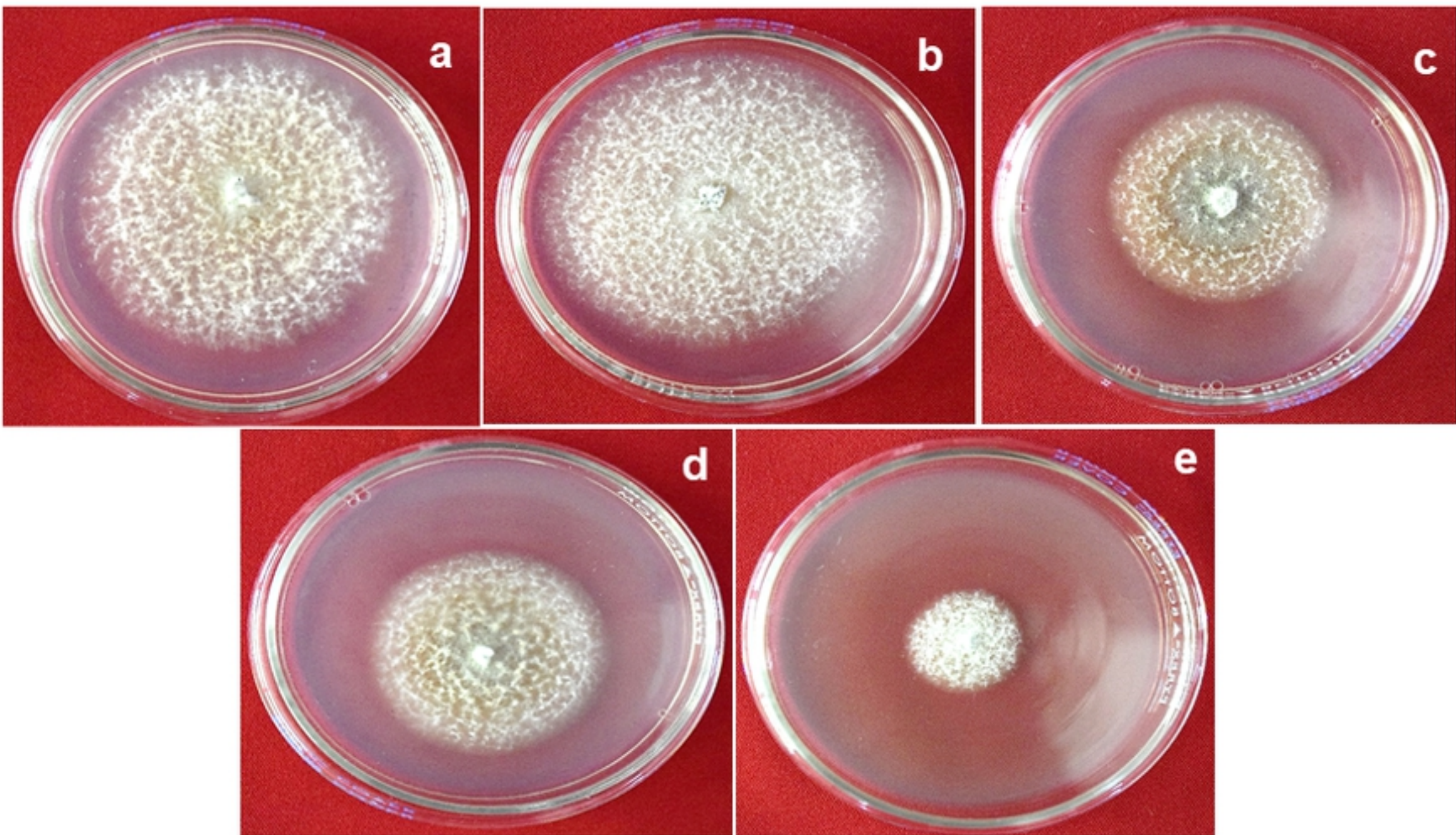


Figure 3

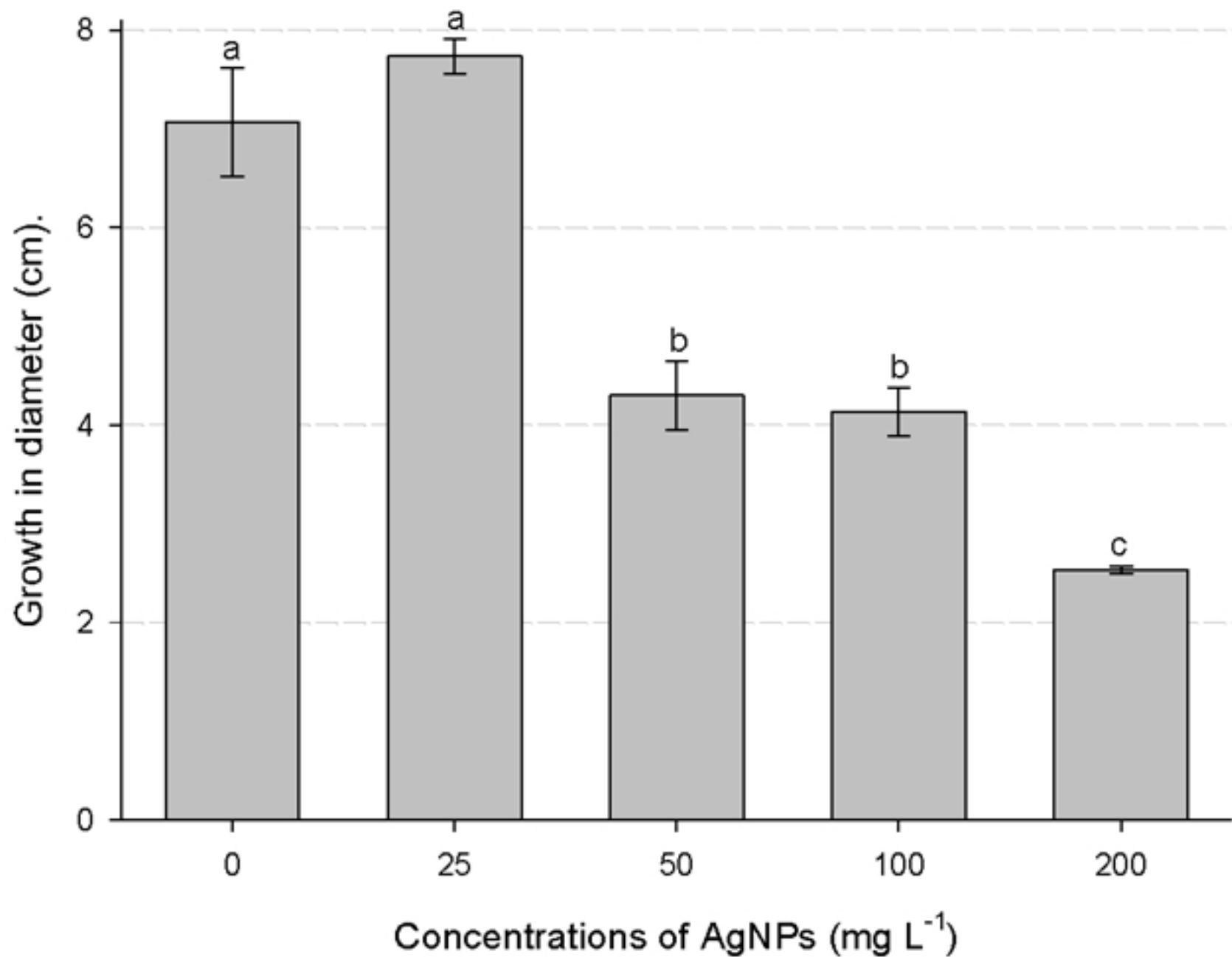


Figure 4

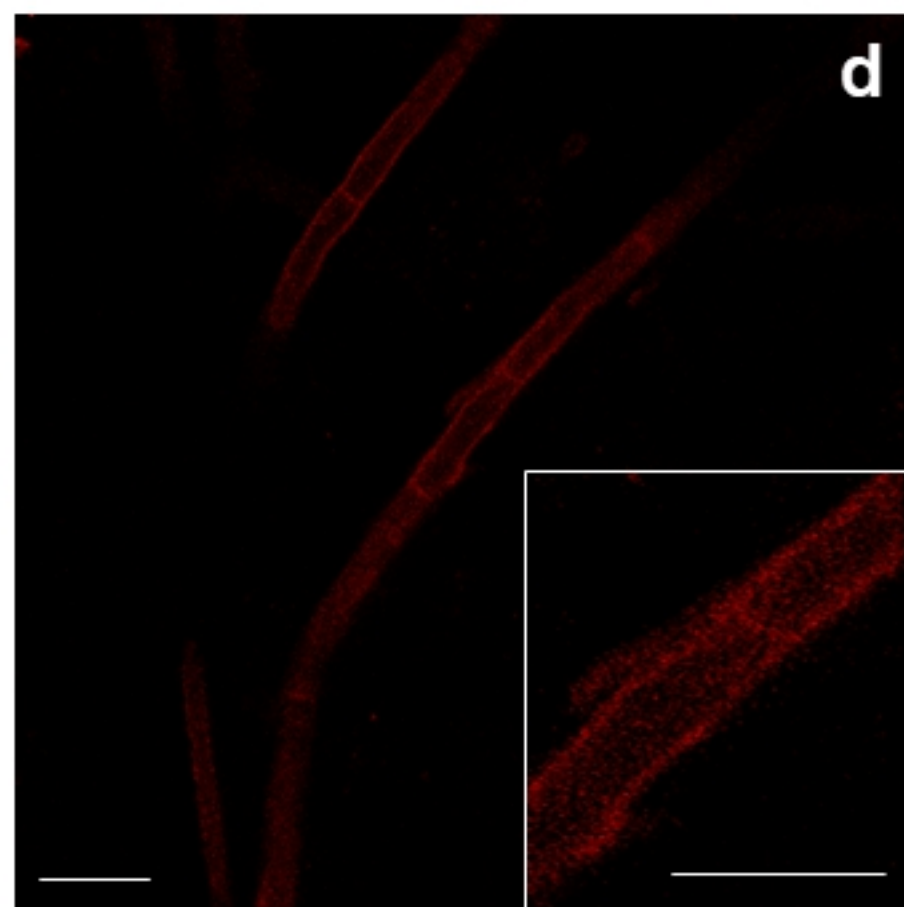
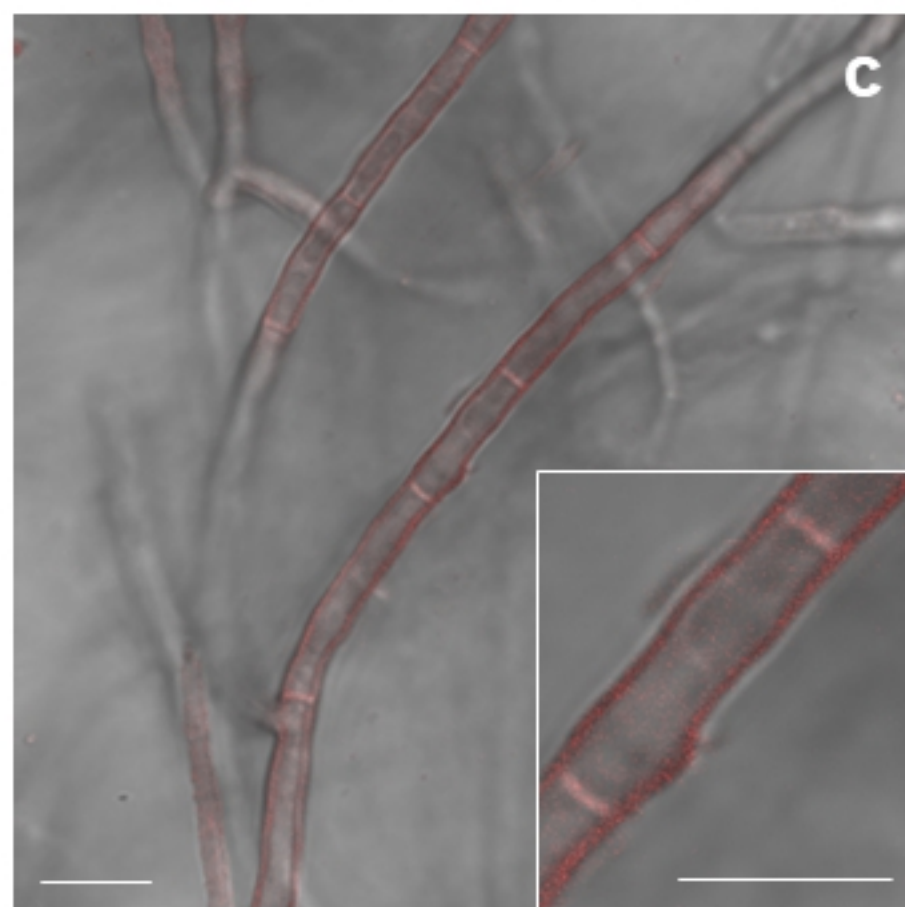
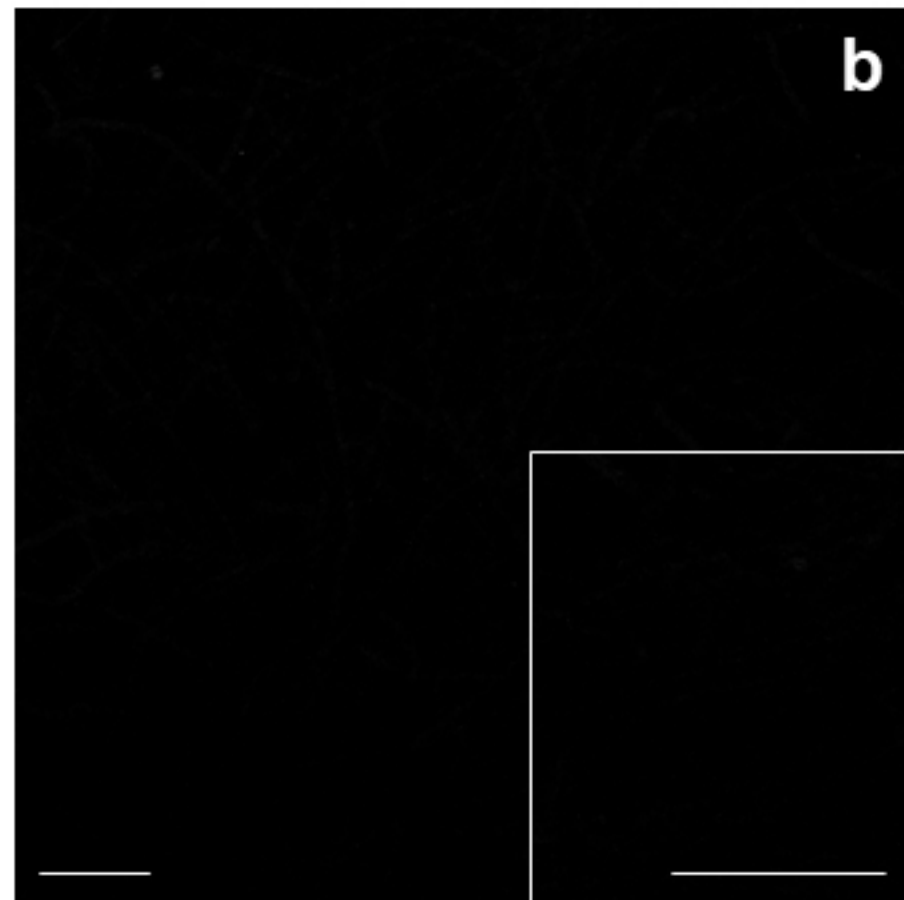
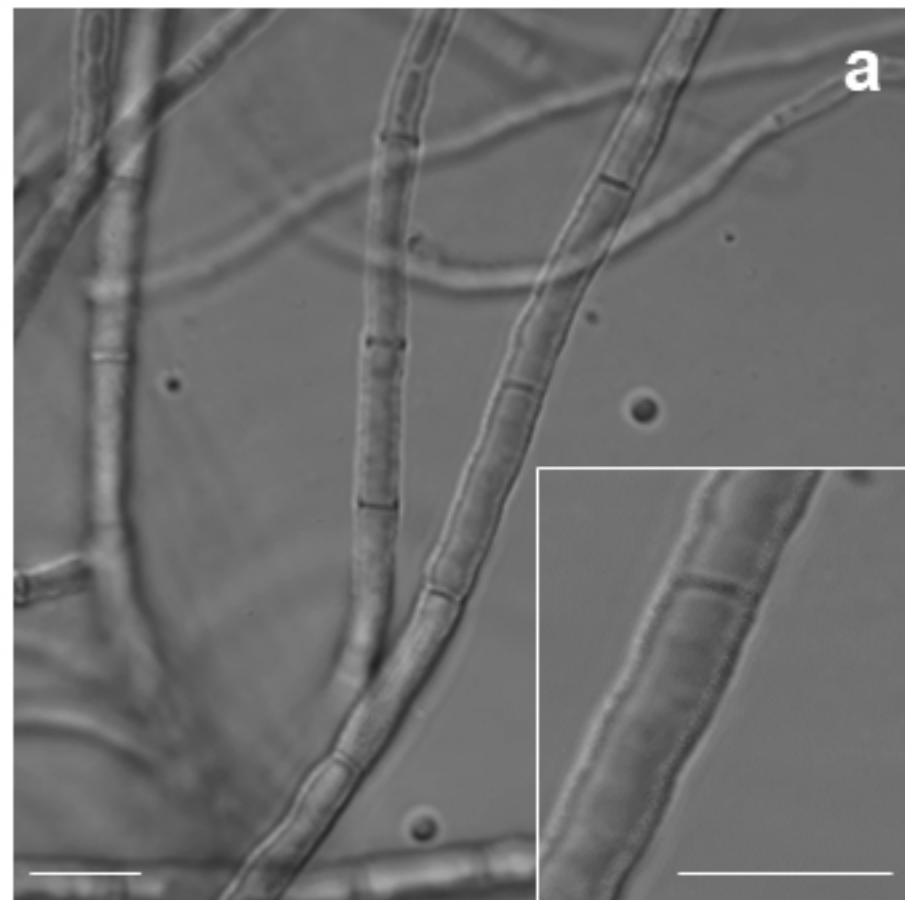


Figure 5